DMD Fast Forward. Published on March 7, 2012 as doi:10.1124/dmd.112.044826

DMD #44826

Generation and characterization of a CYP2A13/2B6/2F1-transgenic mouse model

Yuan Wei, Hong Wu, Lei Li, Zhihua Liu, Xin Zhou, Qing-Yu Zhang, Yan Weng, Jaime D'Agostino, Guoyu Ling, Xiuling Zhang, Kerri Kluetzman, Yunyi Yao, and Xinxin Ding

Wadsworth Center, New York State Department of Health, and School of Public Health, State University of New York at Albany, NY 12201, USA

DMD Fast Forward. Published on March 7, 2012 as DOI: 10.1124/dmd.112.044826
This article has not been copyedited and formatted. The final version may differ from this version.

DMD #44826

RUNNING TITLE: A *CYP2A13/2B6/2F1*-transgenic mouse

ADDRESS CORRESPONDENCE TO:

Dr. Xinxin Ding, Wadsworth Center, New York State Department of Health, Empire State Plaza, Box 509, Albany, NY 12201-0509.

Tel. 518-486-2585; Fax: 518-473-8722; E-mail: xding@wadsworth.org

Number of Text Pages: 23

Number of Tables: 1

Number of Figures: 4

Number of References: 43

Number of words

Abstract: 242

Introduction: 615

Discussion: 1070

ABBREVIATIONS: P450, cytochrome P450; BAC, bacterial artificial chromosome; HPLC, high performance liquid chromatography; RT, reverse transcription; NNK, 4-(methylnitrosamino)-1-(3-pyridyl)-1-butanone; OPB; keto aldehyde; HPB, keto alcohol; O^6-mG, O^6-methyl guanine; LCM, Laser-capture microdissection; bp, base pair; kbp, kilobase pair; WT, wild-type; B6, C57BL/6; TG, CYP2A13/2B6/2F1-transgenic.

DMD Fast Forward. Published on March 7, 2012 as DOI: 10.1124/dmd.112.044826
This article has not been copyedited and formatted. The final version may differ from this version.

ABSTRACT

CYP2A13, CYP2B6, and CYP2F1, neighboring cytochrome P450 (P450) genes on human chromosome 19, are active in the metabolic activation of many drugs, respiratory toxicants, and chemical carcinogens. In efforts to facilitate studies on the regulation and function of these human genes, we have generated a CYP2A13/2B6/2F1-transgenic (TG) mouse (all **1* alleles). Homozygous TG mice are normal in gross morphology, development, and fertility. The tissue distribution of transgenic mRNA expression agreed well with the known respiratory tract-selective expression of CYP2A13 and CYP2F1, and hepatic expression of CYP2B6, in humans. CYP2A13 protein was detected by immunoblot analysis in the nasal mucosa (NM; ~100 pmol/mg microsomal protein; similar to the level of mouse CYP2A5) and the lung (~0.2 pmol/mg microsomal protein), but not in the liver, of the TG mouse. CYP2F1 protein, which could not be separated from mouse CYP2F2 by immunoblot analysis, was readily detected in NM and lung, but not liver, of a TG/*Cyp2f2*-null mouse, at levels 10- and 40-fold, respectively, lower than that of mouse CYP2F2 in the TG mice. CYP2B6 protein was detected in the liver (~0.2 pmol/mg microsomal protein), but not in NM or lung (at a detection limit of 0.04 pmol/mg microsomal protein), of the TG mice. At least one of the transgene (CYP2A13) appears to be active, as NM of the TG mice had greater in vitro and in vivo activities toward bioactivation of a CYP2A13 substrate, 4-(methylnitrosamino)-1-(3-pyridyl)-1-butanone, a lung carcinogen, than did the NM of wild-type mice.

DMD Fast Forward. Published on March 7, 2012 as DOI: 10.1124/dmd.112.044826
This article has not been copyedited and formatted. The final version may differ from this version.

Introduction

The human *CYP2ABFGST* gene cluster on chromosome 19 contains several functional *CYP* genes, which encode five cytochrome P450 (P450) enzymes (CYP2A6, CYP2A13, CYP2B6, CYP2F1, and CYP2S1), as well as several *CYP* pseudogenes (Wang et al., 2003). The five *CYP* genes are all expressed in the respiratory tract, but their contributions to xenobiotic metabolism and target tissue bioactivation remains ill-defined. In order to study the in vivo function as well as regulation of these P450 enzymes, we have been generating transgenic mice that express the cognate human *CYP* genes. We have previously reported the generation and characterization of a *CYP2A6*-transgeic mouse (Zhang et al., 2005a). In the present study, we have prepared a *CYP2A13/2B6/2F1*-transgenic (TG) mouse, mainly for studying the functions of CYP2A13. *CYP2A13* is located ~70 kbp downstream of *CYP2B6* and immediately upstream of *CYP2F1*; all three genes are arranged in the same direction (Fig. 1A). In order to preserve regulatory sequences potentially important for the expression of *CYP2A13*, we selected a human genomic DNA clone encompassing all three *CYP* genes for transgenic mouse production.

CYP2A13, which is preferentially expressed in the respiratory tract, is the most efficient P450 enzyme in the in vitro metabolic activation of 4-(methylnitrosamino)-1-(3-pyridyl)-1-butanone (NNK) (Su et al., 2000; Jalas et al., 2005), a tobacco-specific nitrosamine and potent lung carcinogen (Hecht, 2003). CYP2A13 is also active toward many other toxicants and carcinogens, including aflatoxin B_1 (He et al., 2006), 4-aminobiphenyl (Nakajima et al., 2006), naphthalene, styrene, and toluene (Fukami et al., 2008), and 3-methylindole (D'Agostino et al., 2009). CYP2A13 was hypothesized to play an important

role in NNK-induced lung tumorigenesis (Ding and Kaminsky, 2003). A CYP2A13-transgenic mouse would be valuable not only for directly testing the ability of this human enzyme to mediate chemical carcinogenesis, but also for assessing in vivo efficacy of chemoprevention agents that target CYP2A13.

CYP2B6 is primarily expressed in the liver, where it contributes 2%-10% to total P450 content (Wang et al., 2008). Human CYP2B6 has also been detected, at much lower levels, in several extrahepatic tissues, including brain, kidney, intestine, lung, trachea, nasal mucosa (NM), and skin (Hukkanen et al., 2002; Ding and Kaminsky, 2003; Wang et al., 2008). CYP2B6 metabolizes a large number of substrates, including clinically used therapeutics, recreational drugs, endogenous chemicals, pesticides, and environmental chemicals (Wang et al., 2008).

CYP2F1, which is the least well-characterized of the three human CYPs, is primarily expressed in the respiratory tract (Zhang and Ding 2008; Carlson, 2008; Weems et al 2010). Little CYP2F1 mRNA expression was detected in other tissues (Carr et al., 2003). Studies using mammalian cells containing low levels of heterologously expressed CYP2F1 suggested that CYP2F1 is active toward several pulmonary toxicants, including naphthalene, styrene, 3-methylindole, and benzene (Lanza et al., 1999; Nakajima et al., 1994; Powley et al., 2000); however, heterologous expression of CYP2F1 in non-mammalian systems has yielded non-functional P450 proteins (e.g., Baldwin et al., 2005). Therefore, a CYP2F1-transgenic mouse will be useful for studying the function of CYP2F1 in chemical-induced lung toxicity.

The TG mouse was generally characterized, for viability, growth, and fertility, and then examined thoroughly for tissue distribution of transgene expression, both at the mRNA level and

at protein level. Our results show that *CYP2A13* and *CYP2F1*, but not *CYP2B6*, are expressed in the lung and NM of the TG mouse; whereas CYP2B6 is expressed in the liver of the TG mouse, albeit at very low levels. Furthermore, metabolic studies were conducted, which demonstrated that the transgenic CYP2A13 is capable of bioactivating NNK in vitro as well as in vivo, in the mouse lung. The values, as well as limitations, of this unique transgenic mouse model for studying the in vivo functions of the three human CYPs are also discussed.

DMD Fast Forward. Published on March 7, 2012 as DOI: 10.1124/dmd.112.044826
This article has not been copyedited and formatted. The final version may differ from this version.

Material and Methods

Generation of the TG mouse. A human bacterial artificial chromosome (BAC) clone, ID number CTD-2535H15, containing *CYP2A13*, *CYP2B6*, and *CYP2F1* genes, was obtained from Invitrogen (Carlsbad, CA). The three *CYP* genes in that BAC clone have all been confirmed, through sequence analysis, to be the **1* allele (http://www.cypalleles.ki.se). The ~210-kbp BAC DNA insert (Fig. 1A) was linearized with Not I, which removes the vector, and isolated following pulsed-field gel electrophoresis and β-agarase digestion, according to a published method (Abe et al, 2004). Transgenic mice were produced at the Transgenic and Knockout Core Facility at the Wadsworth Center, according to standard procedures (Nagy et al., 2003). Purified BAC insert was microinjected into the pronuclei of fertilized eggs from the C57BL/6J (B6) strain. The eggs were either transferred the same day, or cultured to the two-cell stage, and then transferred into the oviducts of pseudopregnant B6CBAF1/J mice, and allowed to develop to term. Positive transgenic mice were identified through PCR analysis of tail DNA, with use of the following *CYP2A13*-specific PCR primers: 5'-cctggacagatgcctttaactccg-3' (forward, starting at position +3144 of *CYP2A13*) and 5'-tggctttgcacctgcctgcact-3' (reverse, ending at position +3475) (Zhang et al., 2002). The 332-bp PCR product encompasses *CYP2A13* exon 5.

Heterozygous (+/-) TG mice were intercrossed to obtain homozygotes (+/+). The TG mouse was also crossbred with *Cyp2f2*-null mice (Li et al., 2011); the resultant TG(+/-)/*Cyp2f2*(-/-) mice were used for detection of CYP2F1 protein, without interference by mouse CYP2F2. All studies with mice were approved by the Wadsworth Center Institutional Animal Care and Use Committee.

DMD Fast Forward. Published on March 7, 2012 as DOI: 10.1124/dmd.112.044826
This article has not been copyedited and formatted. The final version may differ from this version.

Southern blot analysis. Mouse genomic DNA was isolated from frozen thymus samples, whereas human genomic DNA was isolated from frozen lung tissues from an 18-year-old African-American male donor (Ling et al, 2007). Hind III-digested genomic DNA was fractionated by electrophoresis on 0.7% agarose gels, transferred to nylon membranes, and analyzed using a ^{32}P-labelled, 864-bp, DNA probe corresponding to *CYP2A13* exon 2 (+593 to +1456). The transgene copy number was estimated, through densitometric analysis of the 5.1-kbp *CYP2A13*-specific band detected. The 1 kb-plus DNA ladder (Invitrogen) was used for size determination.

Quantitative RNA-PCR analysis. Total RNA was isolated using RNeasy Mini kit (Qiagen, Valencia, CA). RNA samples were treated with DNase I (Invitrogen, Carlsbad, CA) before reverse transcription (RT). Real-time RNA-PCR analysis was performed essentially as described previously (Zhang et al., 2007), with primers specific for CYP2A13 (2A13F and 2A13R; Zhang et al., 2004), CYP2F1 (CYP2F1F1 and CYP2F1R1; Zhang et al., 2005b), and CYP2B6 (5'-cattcttccggggatatggtg-3' and 5'-cctcatagtggtcacagagaatcg-3'; Rencurel et al., 2005). Serial dilutions of one RT product were used to generate standard curve. No-template control was used in each reaction. The levels of mouse GAPDH mRNA were also determined as an internal standard (with primers 5'-tgtgaacggatttggccgta-3' and 5'-tcgctcctggaagatggtga-3'; product size: 120 bp).

Laser-capture microdissection (LCM) of lung bronchiolar epithelial cells. Lung tissue samples were prepared from 2-month-old male TG mice. Fresh tissues were mounted in freezing medium and rapidly chilled on dry ice. Frozen sections (10-μm thick) were prepared

DMD Fast Forward. Published on March 7, 2012 as DOI: 10.1124/dmd.112.044826
This article has not been copyedited and formatted. The final version may differ from this version.

with Superfrost/Plus slides (Erie Scientific Company, Portsmouth, NH). Slides were immediately placed in iced 70% ethanol for 10 min, treated with standard H&E staining protocol, and then air-dried for ~10 min before they were used for LCM; the LCM (Pixcell IIe®; Arcturus, Mountain View, CA) procedure was completed within 4 h following slide preparation. Bronchiolar epithelial cells (from distal airway) were isolated with "Arcturus Capsure" caps (Molecular Devices, Sunnyvale, CA). Immediately after LCM, isolated cells were transferred into 0.5-ml LoBind microcentrifuge tubes (Eppendorf North America, Westbury, NY), which were preloaded with 350 μl of a lysis buffer (Qiagen, Valencia, CA). For each lung, ~10,000 cells were captured for RNA preparation.

Immunoblot analysis. Microsomal proteins were prepared from various tissues of 2-month-old mice, as described previously (Ding and Coon, 1990). Monoclonal antibody against human CYP2A6 (A106, BD Gentest, Woburn, MA) was used for detection of CYP2A13 in microsomes prepared from mouse NM. In order to detect CYP2A13 protein in lung microsomes, a rabbit anti-CYP2A5 polyclonal antibody (Gu et al., 1998) was used, and the CYP2A5 and CYP2A13 bands were separated through a high-resolution gel electrophoresis system, as described previously (Wong et al., 2005). Heterologously expressed CYP2A13 in a Sf9 cell microsomal preparation (Su et al., 2000) and purified, recombinant CYP2A5 (Gu et al., 1998) were used as standards for immunoblot quantification.

A CYP2B6-specific monoclonal antibody (BD Gentest) was used for detection of CYP2B6 protein. Recombinant CYP2B6 in a Sf9 cell microsomal preparation (BD Gentest) was used as a standard for immunoblot quantification. A rabbit anti-peptide antibody to CYP2F1/2,

DMD Fast Forward. Published on March 7, 2012 as DOI: 10.1124/dmd.112.044826
This article has not been copyedited and formatted. The final version may differ from this version.

which had been used previously for characterization of the *Cyp2f2*-null mice (Li et al., 2011), was used for detection of CYP2F1 protein in microsomes from TG(+/-)/*Cyp2f2*(-/-) mice. The sequence of the antigenic peptide [NH_2-(C)TPQEFNPEHFLD-COOH; corresponding to amino acids 404-415 of CYP2F1; the first C was added for conjugation] is shared by both CYP2F1 and CYP2F2. The antibody did not cross-react with recombinant CYP1A1, 2A6, 2C9, 2D6, 2E1, 2S1, or 3A4 on immunoblots (data not shown). Heterologously expressed human CYP2F1 protein contained in a Sf9 cell microsomal preparation was used as a positive control for immunoblot analysis. Baculoviral expression of the CYP2F1 protein in Sf9 cells was achieved using the Bac-to-Bac baculovirus expression system (Invitrogen), and a full-length CYP2F1 cDNA entry clone purchased from GeneCopoeia (Rockville, MD). The amount of CYP2F1 protein was not determined; the recombinant CYP2F1 protein did not produce the typical reduced CO-difference P450 spectrum (Omura et al., 1964). For immunoblot analysis of CYP2B6 and CYP2F1, NuPAGE Bis-Tris mini-gels (10%) (Invitrogen, Carlsbad, CA) were used. Calnexin, a marker protein for the endoplasmic reticulum, was detected using a rabbit anti-human calnexin antibody (GenScript), and quantified as a loading control. Prestained protein markers (Precision-Plus, dual color; Bio-Rad, Hercules, CA) were used for size estimation.

Assay for NNK metabolism. In vitro assay for NNK metabolism was performed as described previously (Su et al, 2000), with use of 10 μM NNK (containing 1 μCi [5-^{3}H]NNK for NM microsome or 5 μCi [5-^{3}H]NNK for lung microsome), 5 mM sodium bisulfite, and 0.8

DMD Fast Forward. Published on March 7, 2012 as DOI: 10.1124/dmd.112.044826
This article has not been copyedited and formatted. The final version may differ from this version.

mg/ml (lung) or 0.1 mg/ml (NM) microsomal protein. The rates of formation of the keto aldehyde (OPB) and keto alcohol (HPB) were determined.

Determination of O^6-methyl guanine (O^6-mG) in mouse genomic DNA. Two-month-old mice were treated with a single i.p. injection of NNK (Chemsyn Science Laboratories, Lenexa, KS; dissolved in saline) at 100 mg/kg. Mice were sacrificed 4 h later, and the NM and lungs were obtained for isolation of genomic DNA. O^6-mG levels were determined with a LC-MS method, as described previously (Weng et al., 2007). Female mice were studied, in consideration of their preferred use in NNK-induced lung tumorigenesis studies (e.g., Weng et al., 2007).

DMD Fast Forward. Published on March 7, 2012 as DOI: 10.1124/dmd.112.044826
This article has not been copyedited and formatted. The final version may differ from this version.

Results

Generation of the transgenic mouse model. The structure of the 210-kbp BAC transgene insert is shown in Figure 1A. We selected this clone based on the criteria that the transgene contained the "wild-type" *CYP2A13*1A* allele, and that it retained sufficient amounts of 5'- and 3'-flanking sequences for insulation against potential integration-site effects on the *CYP2A13* transgene expression. Additional genotyping and sequencing analysis indicated that the *CYP2B6* and *CYP2F1* genes were also of the respective **1* alleles and the overall construct contained ~53 kbp at the 5'-end of *CYP2B6*, and ~15 kbp at the 3'-end of *CYP2F1* (Fig. 1A).

We identified two transgenic founder lines (#349 and #864), through PCR-based detection of a 332-bp region containing the *CYP2A13* exon 5 (data not shown). Breeding record suggested that the transgene in line #864, but not that in line #349, was located on the X chromosome, a location that renders it impossible to yield male and female offspring with an equal transgene copy number. Thus homozygous pups from line #349 were used for further studies. The transgenic mice are normal in terms of gross morphology, development, and fertility (data not shown).

We estimated the transgene copy number by Southern blot analysis, with a DNA probe complementary to *CYP2A13* exon 2 and intron 2 (Fig. 1B). As shown in Figure 1C, the most predominant band detected in DNA samples from the transgenic mouse and (as a positive control) in a human lung DNA sample was ~5 kbp, a size consistent with that expected (5.1-kbp) for the positive Hind III fragment (Fig. 1B). The intensity of the ~5-kbp band detected in 2 µg of TG(+/+) genomic DNA was approximately the same as that detected in 10 µg of the human

DMD Fast Forward. Published on March 7, 2012 as DOI: 10.1124/dmd.112.044826
This article has not been copyedited and formatted. The final version may differ from this version.

genomic DNA; this result indicated that the copy number of the transgene was ~5, given the approximately same size of the human and mouse genomes. No bands were detected in 10 µg of genomic DNA from a WT mouse, a result confirming the specificity of the DNA probe used. A second band (~8 kbp in size), weaker than the 5-kbp band, was detected in human (but not TG mouse) DNA samples; this band corresponds to Hind III-fragments from human *CYP2A6* (8.1 kbp) and *CYP2A7* (8.2 kbp). The latter two fragments, which would not be resolved under the experimental conditions used, both contain a region that is 91% identical to the probe sequence (http://www.ncbi.nlm.nih.gov/blast).

An additional, ~6-kbp band, which is ~5-times weaker than the 5-kbp band, was detected in DNA samples from the TG mouse, but not in human lung. This band most likely represents another copy of the transgene, which was truncated at a position downstream of the Hind-III site in the CYP2A13 5'-flanking region (Fig. 1B), and inserted downstream of a Hind-III site in the mouse genome. An alternative explanation, that this band corresponds to a Hind-III fragment (also ~6.0 kbp) from *CYP2A18P-N* (included in the transgene construct), which contains a region that is 84% identical to the probe sequence (http://www.ncbi.nlm.nih.gov/blast), seems less plausible, given that the same 6-kbp band was not detected in the human lung DNA sample.

CYP2A13 expression. CYP2A13 mRNA was detected, by RNA-PCR, in several mouse tissues, including NM, lung, liver, brain, and testis, but essentially not in small intestine, bladder, heart, or kidney; the expression level in the NM was the highest, followed by the lung (Fig. 2A). CYP2A13 protein can be detected with several anti-CYP2A antibodies, which vary in their reactivities with mouse CYP2A proteins. A monoclonal anti-CYP2A6 antibody (Gentest) was

DMD Fast Forward. Published on March 7, 2012 as DOI: 10.1124/dmd.112.044826
This article has not been copyedited and formatted. The final version may differ from this version.

found to have much greater reactivity with CYP2A13 than with mouse CYP2A5 in pilot studies. This antibody was used to detect CYP2A13 protein expression in the NM of the TG mouse. As shown in Figure 2B, CYP2A13 protein was abundantly expressed in the NM; a densitometry analysis of the data shown in Figure 2B (and similar data from additional experiments not presented) suggested that the content of CYP2A13 protein in mouse NM microsomes was ~100 pmol/mg protein, a level similar to that of CYP2A5 protein in mouse NM microsomes determined in a previous study (Gu et al., 1998), and much higher than the levels detected in human fetal or adult NM microsomes (<5 pmol/mg protein; Chen et al., 2003; Wong et al., 2005).

We could not detect CYP2A13 protein in lung microsomes from the TG mouse, when using the monoclonal anti-CYP2A6 antibody (data not shown). However, CYP2A13 protein was detected in the lung (Fig. 2C), when we used a polyclonal anti-CYP2A5 antibody (Gu et al., 1998), which had a much higher titer than the monoclonal antibody did. Notably, the relative band intensities for CYP2A13 and CYP2A5 in the picture shown in Figure 2C (left side) cannot be directly used for a determination of the relative levels of the two CYP2A proteins, because, as shown in the right-side panel, the antibody apparently had greater reactivity toward CYP2A5 than toward CYP2A13. A quantitative analysis indicated that the content of CYP2A13 protein in mouse lung microsomes was ~200 fmol/mg protein, ~10 times higher than the highest levels detected previously in microsomes from human lung biopsy samples (Zhang et al., 2007), although still ~25 times lower than the level of CYP2A5 protein determined in lung microsomes (~5 pmol/mg; data not shown) from homozygous TG mice. In experiments not shown, we also

DMD Fast Forward. Published on March 7, 2012 as DOI: 10.1124/dmd.112.044826
This article has not been copyedited and formatted. The final version may differ from this version.

observed that the levels of CYP2A13 protein in the lung and NM microsomes from male TG mice were ~30% lower than the levels in corresponding tissues from female TG mice.

We also determined the cellular distribution of CYP2A13 mRNA in the lungs of the TG mouse, by RNA-PCR analysis of LCM-isolated lung bronchiolar epithelial cells. We estimated that CYP2A13 mRNA levels (normalized to that of GAPDH) were ~12-fold higher in bronchiolar epithelial cells than in the intact lung (n=4; data not shown). This result agreed well with the findings of a previous immunohistochemical study of CYP2A13 expression in human lung, where the strongest CYP2A13 immunoreactivity was detected in bronchiolar epithelial cells (Zhu et al., 2006).

CYP2A13 protein was not detected in liver microsomes from either male or female TG mice, with a detection limit of ~100 fmol/mg microsomal protein (data not shown). The very low (if any) hepatic expression of CYP2A13 protein in the TG mouse is concordant with the essential lack of CYP2A13 mRNA expression in human liver (Su et al., 2000).

CYP2F1 expression. CYP2F1 mRNA was detected in the transgenic mouse: at the highest levels in the NM and lung; barely detectable in the testis; and undetected in the other tissues examined (Fig. 3A). Efforts to resolve human CYP2F1 and mouse CYP2F2 proteins, using the same high-resolution gel electrophoresis system that was effective for separation of CYP2A13 and CYP2A5, were unsuccessful, and none of the available anti-CYP2F antibodies could distinguish between the two CYP2F proteins (data not shown). Thus, in order to confirm that CYP2F1 protein is produced in the TG mouse, we intercrossed the TG mouse to *Cyp2f2*-null mice (Li et al., 2011), and analyzed microsomes from the TG(+/-)/*Cyp2f2*(-/-) offspring for

DMD Fast Forward. Published on March 7, 2012 as DOI: 10.1124/dmd.112.044826
This article has not been copyedited and formatted. The final version may differ from this version.

CYP2F1 protein expression. As shown in Figure 3B, CYP2F1 protein was readily detected in microsomes from lung and NM, but not liver, of the TG/2f2-null mice. The level of CYP2F1 protein was ~4 times greater in NM than in the lung (densitometry results not shown). A recombinant CYP2F1 protein preparation (CYP2F1 content unknown) was used as a positive control. Notably, although quantitative analysis of the actual amount of CYP2F1 protein detected was not possible, the relative band intensities for CYP2F1 and CYP2F2 can be directly used for a determination of the relative levels of the two CYP2F proteins, given the common presence of the antigenic peptide sequence in the two proteins. Thus, a comparison of the density of the CYP2F2 band detected in WT mice with the density of the CYP2F1 band detected in corresponding tissues of the TG/2f2-null mice indicated that the levels of CYP2F1 protein were ~10 times and ~40 times lower than the levels of mouse CYP2F2 in NM and lung, respectively. In experiments not shown, we observed that there was no noticeable difference in the levels of CYP2F1 protein in lung or NM microsomes from male and female TG/2f2-null mice. CYP2F1 protein was not detected in liver microsomes from male or female TG/2f2-null mice (Fig. 3B and data not shown).

CYP2B6 expression. CYP2B6 mRNA was detected in multiple tissues. The levels were the highest in NM, liver, and kidney; intermediate in small intestine and testis; but barely detected in lung and heart (Fig. 4A). CYP2B6 protein was detected only in liver, at an estimated level of 200 fmol/mg protein (Fig. 4B); it was not detected in NM, lung, small intestine, kidney, brain, or testis, at a detection limit of ~40 fmol/mg protein. There was no sex difference in CYP2B6 protein expression in the liver of the TG mice (data not shown).

DMD Fast Forward. Published on March 7, 2012 as DOI: 10.1124/dmd.112.044826
This article has not been copyedited and formatted. The final version may differ from this version.

NNK bioactivation in lung and NM of the TG mice. Microsomes prepared from lung and NM of WT and TG(+/+) mice were analyzed for their in vitro metabolic activities toward NNK, a CYP2A13 substrate. Formation rates of two stable metabolites of NNK were analyzed. As shown in Table 1, the formation rates of the keto aldehyde (OPB), which represents the α-hydroxylation pathway that leads to O^6-mG DNA adduct formation (Peterson et al., 1993; Hecht, 1998), were significantly increased, compared to WT mice, with both lung and NM microsomes from the TG mice. Formation rates of the keto alcohol (HPB) were also increased, but by smaller extents. These data indicated that the transgenic CYP2A13 or/and CYP2F1 are active in the bioactivation of NNK in vitro. The greater increase in the rates of formation of OPB than in the rate of formation of HPB is consistent with the knowledge that CYP2A13 primarily produces OPB, whereas CYP2A5 preferentially produces HPB (Jalas et al., 2005).

In vivo formation of O^6-mG was also examined in NNK-treated WT and TG mice. At a commonly used NNK dose for lung tumor bioassays (100 mg/kg) (e.g., Weng et al., 2007), NNK-induced O^6-mG formation was significantly increased (by 40%) in the NM of the TG mice, compared to WT mice (Table 1). An apparent increase (by 10%) was also seen in the lung, but the difference was not statistically significant. These in vivo results further confirm that the transgenic CYP2A13 or/and CYP2F1 are active in the bioactivation of NNK. Given a previous report that CYP2F1, heterologously expressed in a mammalian cell system, was a poor catalyst in NNK metabolism (Smith et al., 1992), the increase in NNK bioactivation in the TG mice, compared to WT mice, appeared to be mainly (if not solely) contributed by transgenic

CYP2A13. Therefore, we conclude that the transgenic CYP2A13 is functional in NNK bioactivation, both in vitro and in vivo.

DMD Fast Forward. Published on March 7, 2012 as DOI: 10.1124/dmd.112.044826
This article has not been copyedited and formatted. The final version may differ from this version.

Discussion

In order to accomplish our main goal of achieving adequate, human-like CYP2A13 expression in a mouse model, we considered it necessary to include *CYP2B6* and *CYP2F1* (and the other neighboring *CYP* pseudogenes) in the transgene construct, given their close proximity to *CYP2A13* and the potential for the presence of long-distance and/or shared regulatory elements (such as a locus control region) in a *CYP* gene cluster. For the same reason, the human *CYP1A1* and *CYP1A2* genes had to be co-expressed in a transgenic mouse model (Jiang et al., 2005).

The preferential expression of CYP2A13 and CYP2F1 transgene mRNAs in the respiratory tract is comparable to the respiratory tract-predominant expression reported previously for CYP2A13 (Su et al., 2000; Wong et al., 2005) and CYP2F1 (Carr et al., 2003) transcripts in humans. Notably, it was reported that CYP2A13 is expressed at appreciable levels in human bladders (Nakajima et al., 2006). However, CYP2A13 mRNA levels in the bladders of the TG mice were barely detected. This discrepancy could be due to species differences in the expression of relevant transcription factors in the bladder.

The expression level of transgenic CYP2A13 appeared to be higher than the CYP2A13 levels found in human NM and lung microsomes. This observation may be explained by the fact that the *CYP2A13* transgene existed in multiple copies, and that the quality of mouse tissues was undoubtedly better than that of human biopsy or autopsy samples. Additionally, expression of *CYP2A13* may be suppressed in lung tissues from patients, due to disease-related inflammation (Wu et al., unpublished).

DMD Fast Forward. Published on March 7, 2012 as DOI: 10.1124/dmd.112.044826
This article has not been copyedited and formatted. The final version may differ from this version.

It is interesting to note that, although mouse CYP2A5 and CYP2F2 are both expressed in the liver, as well as in the respiratory tract, human CYP2A13 and CYP2F1 are essentially not expressed in either human liver or in the liver of the TG mouse. This observation indicated that the regulatory sequences responsible for suppressing the expression of CYP2A13 and CYP2F1 in human liver, and/or for activating the expression of CYP2A13 and CYP2F1 in the respiratory tract, are contained within the transgene fragment.

With the exception of CYP2A13 expression in the NM, the levels of expression of the transgenic human CYPs were much lower than the levels of their orthologous mouse P450s. This fact limits the usefulness of the TG mouse for direct analysis of the functions of the transgenic human P450s, as the activities of the mouse P450s will likely mask the activities of the human P450s. Even for CYP2A13 in the NM, the presence of the abundant and highly active mouse CYP2A5 (Su and Ding, 2004) could be problematic; the Km values of recombinant CYP2A5 and CYP2A13 enzymes in OBP formation are similar: 4.3 ± 0.8 μM for mouse CYP2A5 and 3.6 ± 0.7 for human CYP2A13 (Jalas et al., 2005). Nonetheless, the TG mouse can be cross-bred with a suitable *Cyp*-knockout mouse, such as the *Cyp2a5*-null mouse (Zhou et al., 2010), to generate a "humanized" mouse model that expresses human CYP2A13, instead of mouse CYP2A5.

The co-expression of both CYP2A13 and CYP2F1 in the lung and NM of the TG mouse may limit the ability to specifically identify functions for each enzyme. In that regard, efforts are underway to develop additional transgenic mouse models, in which only one of the three human CYPs is expressed. In the case of NNK, previous studies using recombinant human CYP2F1

indicated that, although CYP2F1 could metabolize NNK, its activity was much lower than that of CYP1A2 (Smith et al., 1992), which, in turn, was far less active than CYP2A13 was toward NNK (Jalas et al., 2005). Therefore, the transgenic CYP2F1 is unlikely to make a significant contribution to NNK metabolic activation in the TG mice. Notably, the present TG mouse model will also be useful for studying compounds that are potentially metabolized by both CYP2A13 and CYP2F1, such as 3-methylindole (Lanza et al., 1999; D'Agostino et al., 2009). For these latter compounds, we could still conclude, depending on the data, either 1) that neither enzyme contributes to metabolism/toxicity in the mouse model, or else 2) that both could be important, but further studies are needed to distinguish between their respective contributions (e.g., by using specific inhibitors). These would still be valuable conclusions, considering the current paucity of data regarding in vivo activity of either human P450 enzyme.

CYP2B6 protein was detected, although at a low level, in the liver of the TG mice. The preferential expression of CYP2B6 in the liver of the TG mouse was similar to the expression profile of CYP2B6 in human tissues. It remains to be determined whether, and to what degree, expression of the *CYP2B6* transgene can be induced in the TG mouse by inducers of human *CYP2B6*, such as phenobarbital (Gervot et al., 1999). In humans, *CYP2B6* is highly inducible in the liver, but not in the lung (Hukkanen et al., 2002). Efforts are underway to produce a *CYP2B6*-humanized mouse model, by crossbreeding between the TG mouse described here and a novel *Cyp2* gene cluster-null mouse model (Wei et al., Unpublished) in which all five mouse *Cyp2b* genes are removed.

It should be noted that there were apparent inconsistencies in the relative tissue levels of P450 proteins and P450 mRNAs for CYP2F1 and CYP2B6. Whereas CYP2F1 mRNA levels in NM and lung were not significantly different, its protein level was ~4 times greater in NM than in the lung. Similarly, the mRNA expression of CYP2B6 was comparable between NM and liver; however, CYP2B6 protein was detected only in liver but not in NM. These observations may be explained, at least partly, by tissue- and gene-specific differences in the efficiency of posttranscriptional and/or posttranslational processes that govern the levels of P450 protein expression.

In summary, we have generated a novel transgenic mouse model, in which human CYP2A13 and CYP2F1 are expressed preferentially in the NM and lung, whereas CYP2B6 is expressed in the liver. We further provided evidence indicating that the transgenic CYP2A13 is active toward the lung carcinogen NNK, both in vitro and in vivo. This mouse model should be valuable for a number of applications in molecular toxicology, including studies on 1) the in vivo functions of CYP2A13 and CYP2F1 in xenobiotic metabolism and toxicity in the respiratory tract; 2) in vivo function and regulation of CYP2B6 in the liver; 3) mechanisms of regulation of tissue-specific expression of CYP2A13 and CYP2F1; 4) identification of potential CYP2A13 and CYP2F1 inducers; and 5) determination of in vivo efficacy of CYP2A13 and CYP2F1 inhibitors.

Acknowledgments

We gratefully acknowledge the use of the services of the Biochemistry, Molecular Genetics, and Transgenic and Knockout Mouse Core Facilities of the Wadsworth Center. We thank Dr. Jun Gu for helpful discussion and assistance with LCM; Ms. Ying Liu for assistance with DNA sequence determination; and Ms. Weizhu Yang for assistance with mouse breeding.

Authorship Contributions

Participated in research design: Wei, Wu, Q. Zhang, Kluetzman, and Ding

Conducted experiments: Wei, Wu, Li, Liu, Zhou, Q. Zhang, Weng, D'Agostino, X. Zhang, Kluetzman, Yao

Contributed new reagents or analytic tools: None

Performed data analysis: Wei, Wu, Li, Liu, Zhou, Q. Zhang, X. Zhang, and Ding

Wrote or contributed to the writing of the manuscript: Wei, Wu, Li, Q. Zhang, and Ding

References

Abe K, Hazama M, Katoh H, Yamamura K and Suzuki M (2004) Establishment of an efficient BAC transgenesis protocol and its application to functional characterization of the mouse Brachyury locus. *Exp Anim* **53:**311-320.

Baldwin RM, Shultz MA, and Buckpitt AR (2005) Bioactivation of the pulmonary toxicants naphthalene and 1-nitronaphthalene by rat CYP2F4. *J Pharmacol Exp Ther* **312**:857-865.Carlson G.P. (2008) Critical appraisal of the expression of cytochrome P450 enzymes in human lung and evaluation of the possibility that such expression provides evidence of potential styrene tumorigenicity in humans. *Toxicology* **254**:1–10

Carr BA, Wan J, Hines RN and Yost GS (2003) Characterization of the human lung CYP2F1 gene and identification of a novel lung-specific binding motif. *J Biol Chem* **278:**15473-15483.

Chen Y, Liu YQ, Su T, Ren X, Shi L, Liu DZ, Gu J, Zhang Q-Y, and Ding X (2003) Immunoblot analysis and immunohistochemical characterization of CYP2A expression in human olfactory mucosa. *Biochem Pharmacol* **66**:1245–1251.

D'Agostino J, Zhuo X, Shadid M, Morgan DG, Zhang X, Humphreys WG, Shu YZ, Yost GS and Ding X (2009) The pneumotoxin 3-methylindole is a substrate and a mechanism-based inactivator of CYP2A13, a human cytochrome P450 enzyme preferentially expressed in the respiratory tract. *Drug Metab Dispos* **37:**2018-2027.

Ding X and Coon MJ (1990) Immunochemical characterization of multiple forms of cytochrome P-450 in rabbit nasal microsomes and evidence for tissue-specific expression of P-450s NMa and NMb. *Mol Pharmacol* **37**:489–496.

Ding X and Kaminsky LS (2003) Human extrahepatic cytochromes P450: function in xenobiotic metabolism and tissue-selective chemical toxicity in the respiratory and gastrointestinal tracts. *Annu Rev Pharmacol Toxicol* **43:**149-173.

Fukami T, Katoh M, Yamazaki H, Yokoi T and Nakajima M (2008) Human cytochrome P450 2A13 efficiently metabolizes chemicals in air pollutants: naphthalene, styrene, and toluene. *Chem Res Toxicol* **21:**720-725.

Gervot L, Rochat B, Gautier JC, Bohnenstengel F, Kroemer H, de Berardinis V, Martin H, Beaune P, de Waziers I (1999) Human CYP2B6: expression, inducibility and catalytic activities. *Pharmacogenetics* **9**:295-306.

Gu J, Zhang QY, Genter MB, Lipinskas TW, Negishi M, Nebert DW and Ding X (1998) Purification and characterization of heterologously expressed mouse CYP2A5 and CYP2G1: role in metabolic activation of acetaminophen and 2,6-dichlorobenzonitrile in mouse olfactory mucosal microsomes. *J Pharmacol Exp Ther* **285:**1287-1295.

He XY, Tang L, Wang SL, Cai QS, Wang JS and Hong JY (2006) Efficient activation of aflatoxin B1 by cytochrome P450 2A13, an enzyme predominantly expressed in human respiratory tract. *Int J Cancer* **118:**2665-2671.

Hecht SS (1998) Biochemistry, biology, and carcinogenicity of tobacco-specific N-nitrosamines. *Chem Res Toxicol* **11:**559-603.

Hecht SS (2003) Tobacco carcinogens, their biomarkers and tobacco-induced cancer. *Nat Rev Cancer* **3:**733-744.

Hukkanen J, Pelkonen O, Hakkola J, Raunio H (2002) Expression and regulation of xenobiotic-metabolizing cytochrome P450 (CYP) enzymes in human lung. *Crit Rev Toxicol* **32**:391-411.

Jalas JR, Hecht SS, and Murphy SE (2005) Cytochrome P450 enzymes as catalysts of metabolism of 4-(methylnitrosamino)-1-(3-pyridyl)-1-butanone, a tobacco specific carcinogen. *Chem.Res.Toxicol.* **18**:95-110.

Jiang Z, Dalton TP, Jin L, Wang B, Tsuneoka Y, Shertzer HG, Deka R, Nebert DW (2005) Toward the evaluation of function in genetic variability: characterizing human SNP frequencies and establishing BAC-transgenic mice carrying the human *CYP1A1_CYP1A2* locus. *Hum Mutat.* **25:**196–206

Lanza DL, Code E, Crespi CL, Gonzalez FJ, Yost GS (1999) Specific dehydrogenation of 3-methylindole and epoxidation of naphthalene by recombinant human CYP2F1 expressed in lymphoblastoid cells. *Drug Metab. Dispos* **27**:798–803.

Li L, Wei Y, Van Winkle L, Zhang Q-Y, Zhou X, Hu J, Xie F, Kluetzman K, and Ding X (2011) Generation and characterization of a Cyp2f2-null mouse and studies on the role of CYP2F2 in naphthalene-induced toxicity in the lung and nasal olfactory mucosa. *J Pharmacol Exp Ther* **339**:62-71.

Ling G, Wei Y and Ding X (2007) Transcriptional regulation of human CYP2A13 expression in the respiratory tract by CCAAT/enhancer binding protein and epigenetic modulation. *Mol Pharmacol* **71:**807-816.

Nakajima M, Itoh M, Sakai H, Fukami T, Katoh M, Yamazaki H, Kadlubar FF, Imaoka S, Funae Y and Yokoi T (2006) CYP2A13 expressed in human bladder metabolically activates 4-aminobiphenyl. *Int J Cancer* **119:**2520-2526.

Nakajima T, Elovaara E, Gonzalez FJ, Gelboin HV, Raunio H, Pelkonen O, Vainio H, Aoyama T (1994) Styrene metabolism by cDNA-expressed human hepatic and pulmonary cytochromes P450. *Chem Res Toxicol* **7**:891–896.

Nagy A, Gertsenstein M, Vintersten K, and Behringer R (2003) Manipulating the Mouse Embryo: A Laboratory Manual, 3rd ed, Cold Spring Harbor Laboratory, Cold Spring Harbor, NY

Omura T and Sato R (1964) The carbon monoxide-binding pigment of liver microsomes. I. Evidence for its hemoprotein nature. *J Biol Chem* **230**:2370-8.

Peterson LA, Liu XK and Hecht SS (1993) Pyridyloxobutyl DNA adducts inhibit the repair of O6-methylguanine. *Cancer Res* **53:**2780-2785.

Powley MW, Carlson GP (2000) Cytochromes P450 involved with benzene metabolism in hepatic and pulmonary microsomes. *J Biochem Mol Toxicol* **14**:303–309.

Rencurel F, Stenhouse A, Hawley SA, Friedberg T, Hardie DG, Sutherland C, and Wolf CR (2005) AMP-activated protein kinase mediates phenobarbital induction of CYP2B gene expression in hepatocytes and a newly derived human hepatoma cell line. *J Biol Chem* **280**:4367-4373.

Smith TJ, Guo Z, Gonzalez FJ, Guengerich FP, Stoner GD and Yang CS (1992) Metabolism of 4-(methylnitrosamino)-1-(3-pyridyl)-1-butanone in human lung and liver microsomes and cytochromes P-450 expressed in hepatoma cells. *Cancer Res* **52:**1757-1763.

Su T, Bao Z, Zhang Q-Y, Smith TJ, Hong JY, Ding X (2000) Human cytochrome P450 CYP2A13: predominant expression in the respiratory tract and its high efficiency metabolic activation of a tobacco-specific carcinogen, 4-(methylnitrosamino)-1-(3-pyridyl)-1-butanone. *Cancer Res* **60**:5074-9.

Su T and Ding X (2004) Regulation of the cytochrome P450 2A genes. *Toxicol Appl Pharmacol* **199:**285-294.

von Weymarn LB, Zhang Q-Y, Ding X and Hollenberg PF (2005) Effects of 8-methoxypsoralen on cytochrome P450 2A13. *Carcinogenesis* **26:**621-629.

Wang H, Donley KM, Keeney DS and Hoffman SM (2003) Organization and evolution of the Cyp2 gene cluster on mouse chromosome 7, and comparison with the syntenic human cluster. *Environ Health Perspect* **111:**1835-1842.

Wang H and Thomkins LM (2008) CYP2B6: New insight into a historically overlooked Cytochrome P450 isozyme. *Curr Drug Metab*. **9**:598–610.

Weems, J. M., Lamb, J. G., D'Agostino, J., Ding, X., and Yost, G. S. (2010) Potent mutagenicity of 3-methylindole requires pulmonary cytochrome P450-mediated bioactivation: a comparison to the prototype cigarette smoke mutagens B(a)P and NNK. *Chem. Res. Toxicol*. 23, 1682–1690, 2010

Weng Y, Fang C, Turesky RJ, Behr M, Kaminsky LS, and Ding X (2007) Determination of the role of target tissue metabolism in lung carcinogenesis using conditional cytochrome P450 reductase-null mice. *Cancer Res* **67**:7825-7832.

Wong HL, Zhang X, Zhang Q-Y, Gu J, Ding X, Hecht SS and Murphy SE (2005) Metabolic activation of the tobacco carcinogen 4-(methylnitrosamino)-(3-pyridyl)-1-butanone by cytochrome P450 2A13 in human fetal nasal microsomes. *Chem Res Toxicol* **18:**913-918.

Zhang Q-Y, Gu J, Su T, Cui H, Zhang X, D'Agostino J, Zhuo X, Yang W, Swiatek PJ, Ding X (2005a) Generation and characterization of a transgenic mouse model with hepatic expression of human CYP2A6. *Biochem Biophys Res Commun*. **338**:318-24.

Zhang Q-Y and Ding X (2008) The CYP2F, CYP2G and CYP2J Subfamilies. In *Cytochrome P450: Role in the Metabolism and Toxicity of Drugs and Other Xenobiotics*. (Ioannides C, Ed), Chapter 10, RSC Publishing, Cambridge, UK, pp 309-353.

Zhang XL, Su T, Zhang Q-Y, Gu J, Caggana M, Li H, and Ding X (2002) Genetic polymorphisms of the human CYP2A13 gene: identification of single-nucleotide polymorphisms and functional characterization of an Arg257Cys variant. *J Pharmacol Exp Ther* **302**:416–423.

Zhang X, Caggana M, Cutler TL, and Ding X (2004) Development of a real-time polymerase chain reaction-based method for the measurement of relative allelic expression and identification of CYP2A13 alleles with decreased expression in human lung. *J Pharmacol Exp Ther* **311**:373–381.

Zhang X, Zhang Q-Y, Liu D, Su T, Weng Y, Ling G, Chen Y, Gu J, Schilling B, and Ding X (2005b) Expression of cytochrome P450 and other biotransformation genes in fetal and adult human nasal mucosa. *Drug Metab Dispos* **33:**1423-1428.

Zhang X, D'Agostino J, Wu H, Zhang Q-Y, von Weymarn L, Murphy SE and Ding X (2007) CYP2A13: variable expression and role in human lung microsomal metabolic activation of the tobacco-specific carcinogen 4-(methylnitrosamino)-1-(3-pyridyl)-1-butanone. *J Pharmacol Exp Ther* **323:**570-578.

Zhou X, Zhuo X, Xie F, Kluetzman K, Shu YZ, Humphreys WG and Ding X (2010) Role of CYP2A5 in the clearance of nicotine and cotinine: insights from studies on a *Cyp2a5*-null mouse model. *J Pharmacol Exp Ther* **332:**578-587.

Zhu LR, Thomas PE, Lu G, Reuhl KR, Yang GY, Wang LD, Wang SL, Yang CS, He XY and Hong JY (2006) CYP2A13 in human respiratory tissues and lung cancers: an immunohistochemical study with a new peptide-specific antibody. *Drug Metab Dispos* **34:**1672-1676.

Footnotes

This work was supported in part by the National Institutes of Health National Cancer Institute [Grant CA092596], the National Institutes of Health National Institute of Environmental Health Sciences [Grant ES007462] (to XD), and the National Institutes of Health National Institute of General Medical Sciences [Grant GM074249] (to QZ).

Address correspondence to: Dr. Xinxin Ding, Wadsworth Center, New York State Department of Health, Empire State Plaza, Box 509, Albany, NY 12201-0509. E-mail: xding@wadsworth.org

DMD Fast Forward. Published on March 7, 2012 as DOI: 10.1124/dmd.112.044826
This article has not been copyedited and formatted. The final version may differ from this version.

Legend to Figures

Fig. 1. Structure of the transgene and Southern blot analysis of transgenic mouse. A, Structure of the transgene fragment (Modified from Wang et al., 2003). The ~210-kbp transgene fragment included full-length *CYP2A13*, *CYP2B6* and *CYP2F1* genes, as well as three *CYP2* pseudogenes. B, Strategy for Southern blot analysis. An 864-bp CYP2A13 DNA probe (2A13 probe; open box) was used. Genomic DNA was digested by Hind III. The size of the expected fragment from the *CYP2A13* transgene was 5.1 kbp. C, Southern blot analysis. Increasing amounts (0.1 to 5 μg) of genomic DNA from a homozygous transgenic (TG) mouse were analyzed; genomic DNA from a WT B6 mouse (10 μg) was used as a negative control, whereas human DNA (10 μg) was used as a positive control. The approximate sizes of the detected Hind III fragments are indicated.

Fig. 2. Expression of the *CYP2A13* transgene. A, Relative CYP2A13 mRNA expression levels in various tissues of the TG mice. Total RNA was isolated from tissues of 2-month-old male mice. The values presented (means ± SD; n=4, in arbitrary unit, relative to the highest level detected) were normalized by the levels of mouse GAPDH transcript determined for the same samples. B, Immunoblot detection of CYP2A13 protein in the NM. NM microsomal proteins from 2-month-old WT or homozygous TG mice (male, each sample prepared from pooled tissues from 4 mice), as well as a recombinant CYP2A13 standard, were analyzed using an anti-CYP2A6 monoclonal antibody. The position of a 50-kD prestained protein size marker is indicated. Typical results are shown. C, Immunoblot detection of CYP2A13 protein in the lung. Lung microsomal proteins from 2-momth-old WT or homozygous TG mice (male, each sample

DMD Fast Forward. Published on March 7, 2012 as DOI: 10.1124/dmd.112.044826
This article has not been copyedited and formatted. The final version may differ from this version.

prepared from pooled tissues from 4 mice), as well as recombinant CYP2A5 and CYP2A13 standards at indicated amounts, were analyzed using a polyclonal anti-CYP2A5. Typical results are shown.

Fig. 3. Expression of the *CYP2F1* transgene. A, Relative CYP2F1 mRNA expression levels in various tissues of the TG mice. Total RNA was isolated from tissues of 2-month-old male mice. The values shown (means ± SD; n=4, in arbitrary unit, relative to the highest level detected) were normalized by the levels of mouse GAPDH transcript determined for the same samples. B, Immunoblot detection of CYP2F1 and CYP2F2 proteins. Lung, liver, and NM microsomal proteins from 2-month-old female WT, *Cyp2f2*-null, and TG(+/-)/*Cyp2f2*-null mice (each sample prepared from pooled tissues from 4~5 mice) were analyzed, using an anti-CYP2F1/2 antibody. A recombinant CYP2F1 protein sample (in Sf9 cell microsomes) was used as a positive control. Typical results are shown.

Fig. 4. Expression of the *CYP2B6* transgene. A, Relative CYP2B6 mRNA expression levels in various tissues of the TG mice. Total RNA was isolated from tissues of 2-month-old male mice. The values presented (means ± SD; n=4, in arbitrary unit, relative to the highest level detected) were normalized by the levels of mouse GAPDH transcript determined for the same samples. B. Immunoblot detection of CYP2B6 protein. Microsomal proteins prepared from tissues pooled from three 2-month-old male homozygous TG mice, and a recombinant CYP2B6 standard (in Sf9 cell microsomes), were analyzed using an anti-CYP2B6 antibody. Typical results are shown.

DMD Fast Forward. Published on March 7, 2012 as DOI: 10.1124/dmd.112.044826
This article has not been copyedited and formatted. The final version may differ from this version.

TABLE 1

NNK metabolic activation in the lung and NM of WT and TG mice

NNK metabolism in microsomal reactions and NNK-induced O^6-mG formation in vivo were assayed as described in Materials and Methods. Rates of keto aldehyde and keto alcohol formation (mean ± SD, n=3) were determined, with NNK at 10 μM. Each microsome sample (three per group) was prepared from pooled tissues of four 3-month-old male mice. For DNA adduct analysis, tissues were obtained at 4 h after NNK treatment (at 100 mg/kg, i.p.). The O^6-mG/guanine ratios (mean ± S.D., n=4) were determined for 2-month-old female mice. Values in parentheses indicate relative increases in TG vs. WT mice.

Tissue	Strain	Product formation in vitro		DNA adduct formation in vivo
		Keto aldehyde	Keto alcohol	
		pmol/min/mg protein		*O^6-mG/10^6 guanine*
Nasal mucosa	WT	275 ± 53	388 ± 80	309 ± 10
	TG	597 ± 12[a] (220%)	575 ± 46[b] (150%)	439 ± 40[a] (140%)
Lung	WT	2.9 ± 0.4	16.2 ± 2.2	11.4 ± 0.8
	TG	5.7 ± 0.4[a] (200%)	19.8 ± 4.0 (120%)	13.0 ± 0.3 (110%)

[a] $p < 0.01$, compared with WT mice (Student's *t* test)

[b] $p < 0.05$, compared with WT mice (Student's *t* test)

DMD Fast Forward. Published on March 7, 2012 as DOI: 10.1124/dmd.112.044826
This article has not been copyedited and formatted. The final version may differ from this version.

Fig. 1

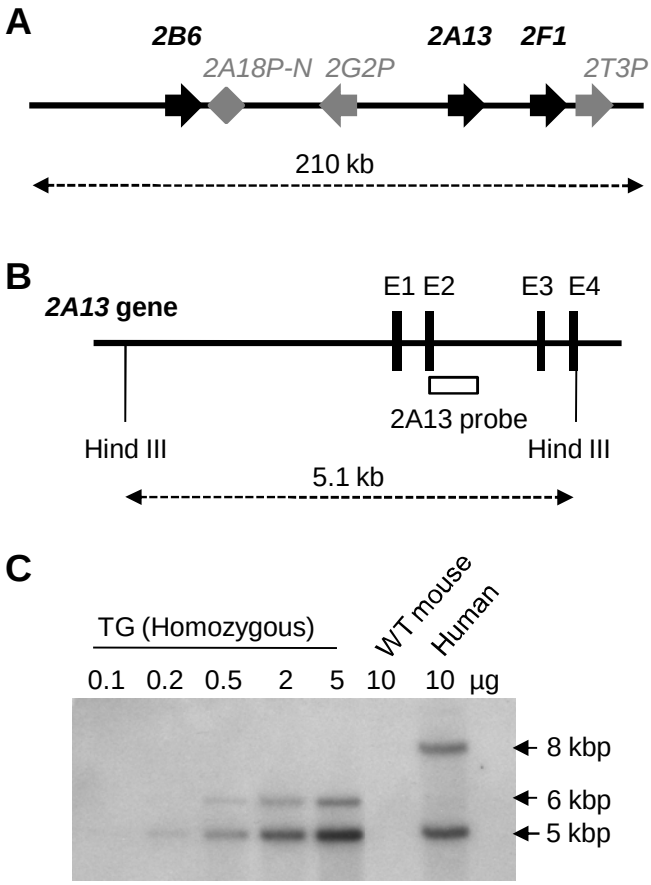

DMD Fast Forward. Published on March 7, 2012 as DOI: 10.1124/dmd.112.044826
This article has not been copyedited and formatted. The final version may differ from this version.

Fig. 2

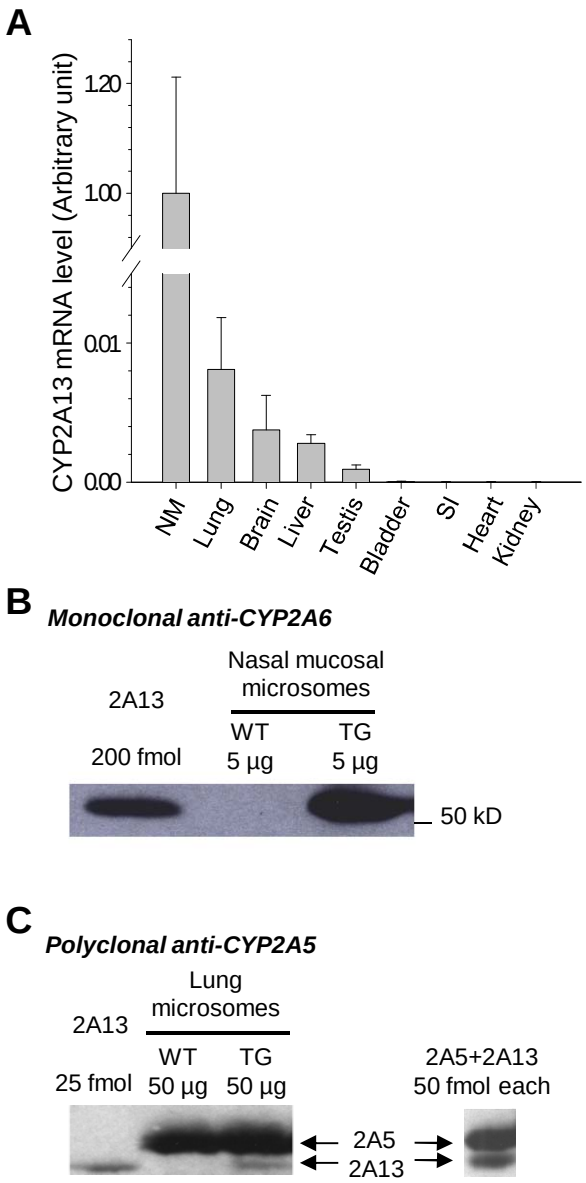

DMD Fast Forward. Published on March 7, 2012 as DOI: 10.1124/dmd.112.044826
This article has not been copyedited and formatted. The final version may differ from this version.

Fig. 3

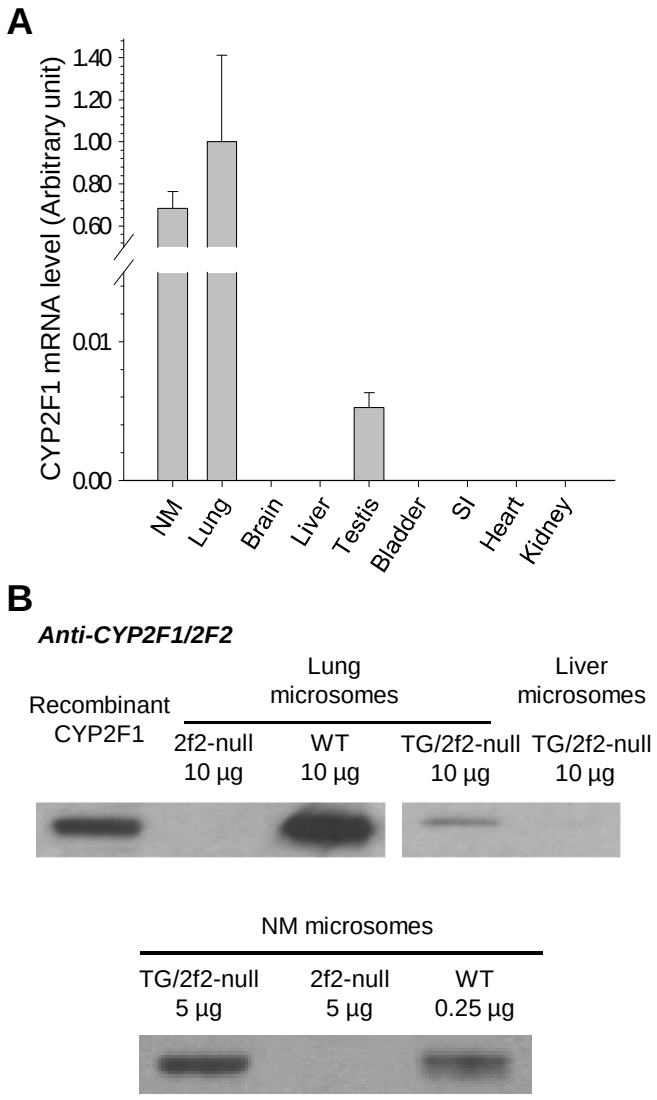

DMD Fast Forward. Published on March 7, 2012 as DOI: 10.1124/dmd.112.044826
This article has not been copyedited and formatted. The final version may differ from this version.

Fig. 4